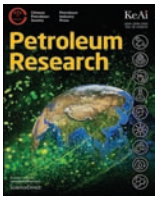
Petroleum Research 11 (2026) 63–71

Contents lists available at ScienceDirect

Petroleum Research

journal homepage: http://www.keaipublishing.com/en/journals/petroleum-research/



Full Length Article

Correlation-based EUR prediction of shale oil wells: A case of the Qingcheng Oil Field in the Ordos Basin

Suiyi Fu [a], Lingbin Lai [b], Zhengdong Lei [b], Qingfu Feng [b], Huizhu Xiang [b, *], Bo Wang [c], Xiulin Hou [b], Ting Xue [c]

[a] Halliburton (China) Energy Services Limited, Beijing, 100020, China
[b] Research Institute of Petroleum Exploration and Development, PetroChina, Beijing, 100083, China
[c] PetroChina Changqing Oilfield Company, Xi'an, 710000, China

ARTICLE INFO

Article history:
Received 22 October 2024
Received in revised form
29 May 2025
Accepted 3 June 2025
Available online 7 June 2025

Keywords:
Shale reservoirs
Estimated ultimate recovery
Production decline
Qingcheng Oil Field

ABSTRACT

Shale reservoirs are characterized by low permeability and a weak capacity for natural seepage. These reservoirs are commonly developed using a combination of horizontal well drilling and fracturing. The production performance of shale oil wells is evaluated through single-well production decline analysis, with the estimated ultimate recovery (EUR) used as an important indicator of the development outcome. This study predicted the EUR of the X233 well zone in the Qingcheng Shale Oil Field in the Ordos Basin. It reviewed the applicability of production forecasting methods to unconventional reservoirs and put forward a correlation-based approach to EUR prediction. The latter was developed by integrating the characteristics of Qingcheng shale oil production with EURs predicted using empirical methods intended for typical wells. The correlation-based approach was also designed on the basis of the relationship between cumulative oil production and the empirically derived EURs. The results suggest that the proposed method rapidly predicts the EUR of a single well using cumulative oil production from the first one, two, and three years of production. The predictions closely align with the empirically derived values, demonstrating the strong practical effectiveness of the approach put forward in this work. To determine its applicability and limitations, this study examined the EUR distribution characteristics of different well classes (Classes I to III). This research provides a simple and effective approach to rapidly predicting the EURs of shale oil wells, significantly reducing computational time and labor costs.

© 2025 Chinese Petroleum Society. Publishing services by Elsevier B.V. on behalf of KeAi Communications Co. Ltd. This is an open access article under the CC BY-NC-ND license (http://creativecommons.org/licenses/by-nc-nd/4.0/).

1. Introduction

China possesses abundant shale oil resources, which are distributed primarily across the Songliao, Ordos, Junggar, and Sichuan Basins. These resources are of strategic importance and serve as critical supplements to national energy security. Currently, they are predominantly developed using horizontal well drilling combined with hydraulic fracturing. To accurately estimate the amount of oil that can be economically and efficiently extracted from shale oil wells under current technological conditions, it is necessary to predict the maximum estimated ultimate recovery (EUR) of these sites. The problem is that EUR forecasting for unconventional fields has been a difficult process because of the physics principles involved in the production mechanisms of such systems; that is, these principles render modeling or prediction challenging.

The current major approaches to EUR prediction are empirical, analytical, and numerical methods. First, empirical methods are used to predict EUR on the basis of historical production data and empirical formulas. These methods are generally simple and easy to use but rely on assumptions and empirical parameters, making them suitable for reservoirs for which limited data have been accumulated or reservoirs in the early stages of development. An example is Arps's (1945) decline curve analysis (DCA), which is a classical method that predicts future production and EUR by fitting production data to decline curves (exponential, hyperbolic, or

* Corresponding author. Research Institute of Petroleum Exploration and Development, PetroChina, Beijing, 100083, China.
E-mail address: xhz2022@petrochina.com.cn (H. Xiang).
Peer review under the responsibility of Editorial Office of Petroleum Research.

https://doi.org/10.1016/j.ptlrs.2025.06.001
2096-2495/© 2025 Chinese Petroleum Society. Publishing services by Elsevier B.V. on behalf of KeAi Communications Co. Ltd. This is an open access article under the CC BY-NC-ND license (http://creativecommons.org/licenses/by-nc-nd/4.0/).

harmonic decline). DCA is the preferred method for predicting the producton rate, decline rate and EUR of unconventional wells (Acuña, 2021; Artus and Houzé, 2018). However, conventional Arps models are confronted with problems when wells exhibit extended transient flow behavior, prompting the development of logistic growth models (Clark et al., 2011). The limitations of Arps models in applications involving unconventional reservoirs have also been addressed using the Duong model (Duong, 2010, 2021) and the stretched exponential production decline (SEPD) model (Valko, 2009).

Second, analytical methods of EUR forecasting are based on reservoir engineering theories and mathematical models, and they use reservoir flow mechanics and material balance principles to generate predictions. These methods are more physically rigorous than empirical approaches, but they typically require more input parameters. For example, Patzek et al. (2013) constructed a physics-based analytical model that can obtain the upper and lower bounds of the gas produced by a shale gas well. More recently, Ruiz Maraggi et al. (2024) developed an analytical model specifically for the examination of production under variable BHP (Bottom hole pressure). Despite the insights derived from these approaches, however, the latest analytical methods are unpopular since they generate only rough approximations of EUR given the uncertainty in reservoir properties and the requirement for reliable pressure data. In addition, the need for large quantities of input data and their complexity pose challenges to the practical application of these methods.

Finally, numerical methods of EUR prediction involve constructing reservoir models and simulating production dynamics using computational tools. These approaches are highly accurate but computationally intensive. Recent years have seen the emergence of data-driven numerical methods based on machine learning, which predict EUR by training models on relationships between production data and geological parameters (Ibrahim et al., 2023; Mehana et al., 2019; Temizel et al., 2021; Wang et al., 2022).

To address these challenges, this study introduces a rapid, correlation-based method for estimating the EUR of shale oil wells using cumulative production data from the first one to three years. Validated in the X233 block of the Qingcheng Oil Field, this approach streamlines the prediction process, reduces computational effort, and delivers results comparable to more complex empirical models. By relying solely on readily available production data, it removes the need for multiple reservoir parameters, enabling efficient and timely decision-making—particularly in early development stages or data-limited settings. This method therefore bridges empirical tradition and modern data-driven needs, supporting standardized EUR estimation and informing both field development planning and resource evaluation.

2. Geological setting

The Qingcheng Oil Field is located in the southwestern part of the Yishan Slope in the Ordos Basin (Fig. 1). The shale oil in the Chang 7 Member of the Upper Triassic Yanchang Formation is a representative example of the lacustrine shale oil found in China (Niu et al., 2022). This formation consists of semideep to deep lacustrine fine-grained deposits with a stratigraphic thickness of approximately 110 m. From bottom to top, it is further divided into the Chang 7_3, Chang 7_2, and Chang 7_1 submembers.

The sand and mud interbedding in the Chang 7 Member are influenced by hydrodynamic conditions and the undulating geomorphology of the lake basin, and the reservoir is highly heterogeneous in both the vertical and lateral directions (Xue et al., 2021). The sedimentary structures in this member are well developed and diverse, encompassing commonly occurring features such as mudstone detachment structures, convolute deformation bedding, sand pillow structures, load casts, flame structures, and groove casts. Coal fragments and fish scale fossils are also frequently observed in mudstone and silty mudstone (Fig. 2).

At present, Chang 7_2 and Chang 7_1 are the main strata for development in the oil field. The reservoir depth is 1750–2030 m, the formation pressure is 14.7–15.8 MPa, and the pressure coefficient is 0.77–0.82. The average porosity of the reservoir is 9.2%, and its average permeability is 0.10 mD. The original gas-to-oil ratio ranges from 70 to 120 m^3/t, while the average viscosity is 1.35 mPa s. The pore radius is primarily concentrated in the range of 2–8 μm, with throat sizes ranging from 20 to 100 nm. Chang 7 in the Yanchang Formation is currently one of the key areas for exploration and development in China (Ju et al., 2023). Since 2011, the development of the Qingcheng Shale Oil Field has undergone three stages: evaluation and exploration, development and testing, and demonstration and construction. A demonstration area for million-ton shale oil field development has now been established (Xue et al., 2021).

3. Methods of predicting shale oil production

3.1. Overview of prediction methods for unconventional reservoirs

Production decline analysis can be conducted to evaluate the decline patterns of oil wells and estimate their EURs. With the development of shale reservoirs, methods for analyzing decline have been widely applied to shale oil production and EUR evaluation. The main approaches intended for unconventional reservoirs include Arps models, hyperbolic plus, the Duong model, Duong + hyperbolic, YM-SEPD (Yu-Miocevic Stretched Exponential Production Decline), YM-SEPD + hyperbolic, YM-SEPD for SH, and YM-SEPD (SH) + hyperbolic. These are underlain by varying basic principles and applicable conditions (Table 1).

3.2. Characteristics of Qingcheng shale oil production

As shown in Fig. 3, the production process of Qingsheng shale oil can be divided into three stages: production ramp-up, rapid decline, and slow decline. In the production ramp-up stage (months 0–6), liquid production decreases, while oil production increases. In the rapid decline stage (months 7–44), annual oil production declines by approximately 20.8%, and annual liquid production declines by approximately 25.2%. In the slow decline stage (month 45 onward), annual oil and liquid production declines by approximately 11.5% and 11.3%, respectively.

3.3. EUR prediction via empirical methods

The diagnostic curve (the log-log plot of normalized production versus time) and the characteristic curve (the plot of normalized pressure versus the square root of material balance time) from the Wattenbarger model (Ei-Banbi and Wattenbarger, 1998; Hui et al., 2017; Wattenbarger et al., 1988) are used to identify the flow regimes of multistage fractured horizontal wells. When the pseudo-steady-state flow phase is reached, the diagnostic curve exhibits a straight-line segment with a slope of −1, and the characteristic curve deviates from the initial straight-line segment and begins to bend upward.

Normalized production:

$$\frac{q_o}{\Delta p} = \frac{q_0}{P_i - P_{wf}} \tag{1}$$

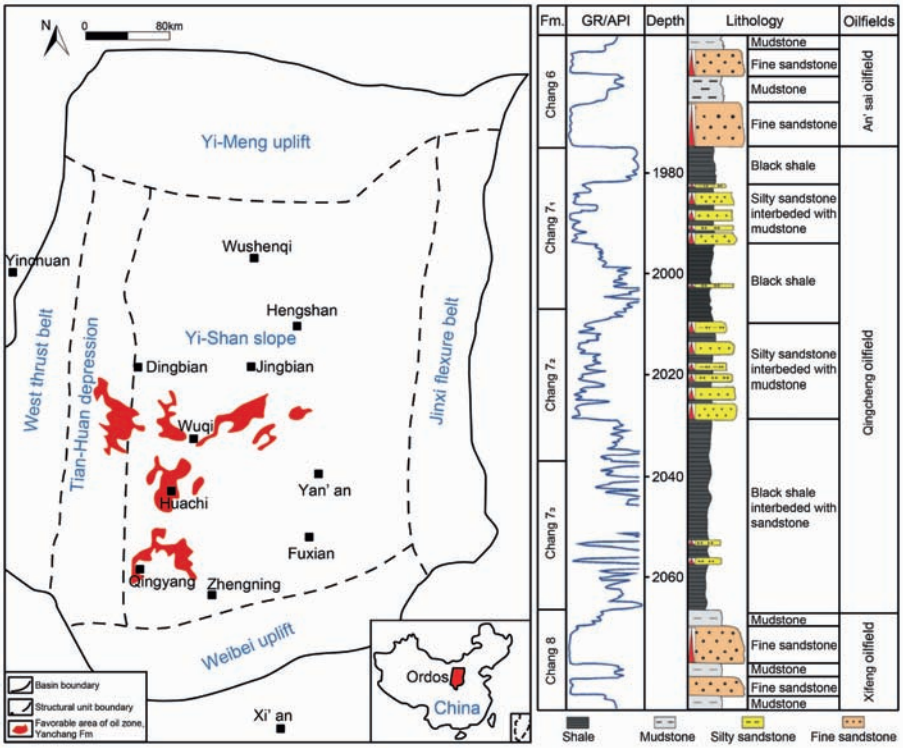


Fig. 1. Distribution of favorable oil zones and and the stratum profile of the Yanchang Formation in the Ordos Basin (Xue et al., 2021).



Fig. 2. Structure of sediment in the Chang 7 Member, Qingcheng Oil Field.

Normalized pressure:

$$\frac{\Delta p}{q_o} = \frac{P_i - P_{wf}}{q_0} \tag{2}$$

In the equations above, P_i is the original reservoir pressure (MPa), P_{wf} denotes the pressure at the well bottom (MPa), and q_o represents daily oil production (m^3/d).

As shown in Fig. 4, the characteristic curve of well A1 exhibits an inflection point after $\sqrt{d} = 30$, and the derivative of the normalized pressure on the diagnostic curve in Fig. 5 shows a slope of -1. Therefore, the well enters a boundary-dominated pseudo-steady-state flow after 900 days.

On the basis of the time at which well A1 reaches the pseudo-steady-state flow, as indicated by the diagnostic and characteristic curves, the hyperbolic method ($b < 1$) or the YM-SEPD approach was used to predict EUR after the pseudo-steady-state flow was reached (Fig. 6). For EUR prediction during the transient flow phase, the Duong + YM-SEPD method was applied (Fig. 7).

A total of 110 horizontal wells in the X233 well zone of the Qingcheng Oil Field were selected for the analysis, and the single-well EUR was predicted using the empirical methods mentioned above. The initial daily oil production (i.e., production in the first three months after the water cut drops to 60%) of the horizontal wells was also recorded. As shown in Fig. 8, the EUR is linearly

Table 1
Applicability of prediction methods for shale oil production.

Classification	Number	Prediction method	Fundamentals	Application requirement		
				Permeability/mD	Production/year	Applicability
Empirical methods	1	Arps	According to the statistical study of field data, when oil and gas field production enters the decline stage, its decline rate is equal to the change rate of production per unit of time (Li, 2013), which is classified as exponential decline, hyperbolic decline, and reconciled decline according to the decline index.	Unrestricted		Reaching boundary-controlled pseudo-steady flow
	2	Hyperbolic plus	The hyperbolic + hyperbolic decline model was introduced by Yu (2018), and it fits the historical production data in the first half of the period using a first-stage hyperbolic decline. When a key point in time is reached or the decline rate drops to a lower limit, it switches to a second-stage hyperbolic decline for long-term forecasting. This allows the predicted production curve to be smoother and more accurately reflect actual production history.	$>10^{-3}$	>2	/
	3	Duong (2010, 2011)	On the basis of the analysis of the production history of numerous Barnett shale gas wells in the United States, Duong (2010, 2011) concluded that the production history of gas wells after hydraulic fracturing exhibits a fractured linear flow over a long period. This phenomenon can be expressed as $q/G_p = at^{-m}$.	$<10^{-3}$ 10^{-3}–10^{-2} 10^{-2}–10^{-1}	>3–4 3–4 2–3	Suitable for early unsteady linear flow; unsuitable for fitting an entire production history, which would otherwise overestimate the production of horizontal wells (Yu, 2018)
	4	Duong + hyperbolic	To take advantage of the Duong model's effectiveness in accurately predicting unsteady linear flow production and avoid optimistically predicting production when production characteristics do not correspond with unsteady linear flow, Joshi and Lee (2013) used a combined Duong and hyperbolic approach: When the production history deviates from the linear flow straight-line inflection point, the hyperbolic decline model is used for prediction. Yu (2013) conducted a numerical simulation to derive the applicability conditions of the model. Lee established formulas for calculating the decline rate and decline exponent of hyperbolic decline from the parameter values of the Duong model (a, m) at a given point in time in the SPEE monograph (Seidle et al., 2016).	$<10^{-3}$ 10^{-3}–10^{-2} 10^{-2}–10^{-1}	>3–4 3–4 2–3	Being able to predict the complete production history of oil and gas wells reasonably or conservatively (Yu, 2018).
	5	YM-SEPD (Zhang et al., 2016)	Valko (2009) proposed the SEPD method, which focuses mainly on analyzing the production history of many single wells and well groups in Barnett shale gas fields. Later, Kabir et al. (2011) applied this model to the prediction of production in shale oil reservoirs. When the EUR is unknown, it is difficult to calculate n and τ accurately using the SEPD method. To solve this problem, Yu (2013) derived an improved SEPD method based on the original and called it the YM-SEPD method.	$<10^{-3}$ 10^{-3}–10^{-2} 10^{-2}–10^{-1}	>3–4 3–4 2–3	Production histories with multiple flow characteristics can be fitted, but when production histories are short, model predictions are conservative (Yu, 2018).
	6	YM-SEPD + hyperbolic	To solve the problem of conservative SEPD prediction results under a short production history (Yu, 2013), the YM-SEPD + hyperbolic model was introduced on the grounds of the hyperbolic + hyperbolic decline model (Statton, 2011). The YM-SEPD method was used to predict production at the	$<10^{-3}$ 10^{-3}–10^{-2} 10^{-2}–10^{-1}	>3–4 3–4 2–3	/

Table 1 (*continued*)

Classification	Number	Prediction method	Fundamentals	Application requirement		
				Permeability/mD	Production/year	Applicability
			unsteady flow stage, and the hyperbolic decline of the Arps decline model was applied after boundary flow was reached.			
	7	YM-SEPD for SH (Zhang et al., 2016)	Examples show that when reservoir permeability is less than 0.1 mD and the production history of a well is less than 2 years, the Duong method can accurately predict a "proposed" history of 3–4 years. With 3–4 years of production history as a basis, the YM-SEPD method can reliably and reasonably predict relatively conservative production and recoverable reserves. As a result, Yu et al. (2018) combined the YM-SEPD and Duong methods; for wells with less than 2 years of production history, they first used the Duong method to predict 3–4 years of "proposed" history, after which they applied YM-SEPD to predict the production and recoverable reserves of a single well based on 3–4 years of data.	10^{-3}–10^{-2} 10^{-3}–10^{-1}	4 3	Actual production history <2 years
	8	YM-SEPD (SH) + hyperbolic	The YM-SEPD (SH) + hyperbolic decline model supplements YM-SEPD for the SH method with a decline analysis approach intended for oil and gas wells in shale formations after boundary flow is reached, during which the hyperbolic decline in the Arps decline model is also applied.	10^{-3}–10^{-2} 10^{-3}–10^{-1}	4 3	Actual production history <2 years
Analytical method (Yu, 2018)			The Wattenbarger model for multistage fractured horizontal wells was developed, and the production and pressure data were fitted to calculate fracture parameters, such as the half-length of fracture and conductivity, which were combined with well spacing to carry out EUR prediction.	/	>1	/

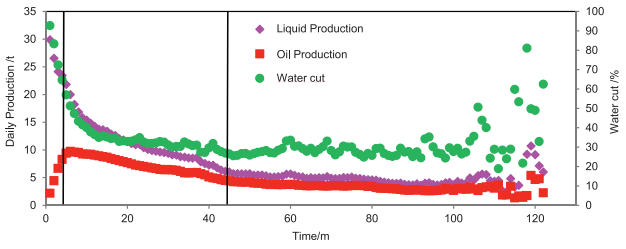


Fig. 3. Characteristics of Qingcheng shale oil production.

correlated with the initial daily oil production—the higher the initial daily oil production, the greater the EUR.

The initial daily oil production was used as a basis for classifying the horizontal wells into three categories: Class I wells (initial daily oil production >16 t), Class II wells (10 t < initial daily oil production ≤16 t), and Class III wells (initial daily oil production ≤10 t). In accordance with the linear correlation between the EUR and the initial daily oil production, Classes I, II, and III have average EURs of 3.18×10^4 t, 2.58×10^4 t, and 1.08×10^4 t, respectively.

4. Results

The relationship between the empirical EURs and cumulative oil production for Classes I to III was established using the classification of

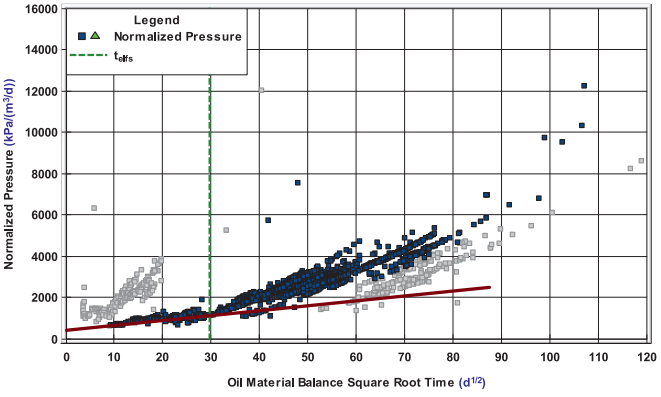


Fig. 4. Characteristic curve of well A1.

110 horizontal wells in the X233 well zone of the Qingcheng Oil Field as well as the cumulative oil production one, two, and three years after production began. The data were employed in developing the correlation-based method for predicting EURs for these well classes.

4.1. Relationship between cumulative oil production and EUR: class I

Figs. 9–11 illustrate the relationship between cumulative oil production at different periods and the empirical EUR of the Class I wells.

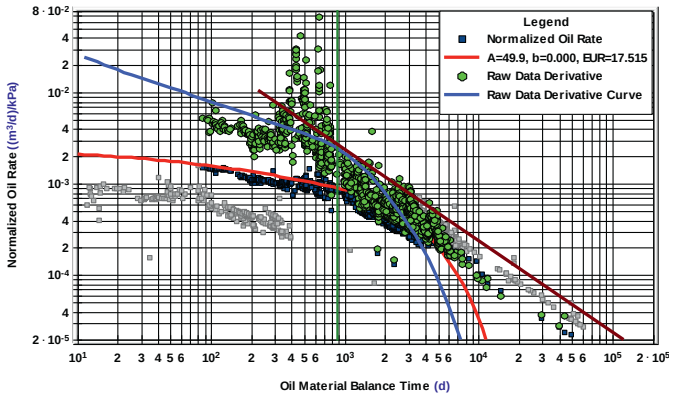


Fig. 5. Diagnostic curve of well A1.

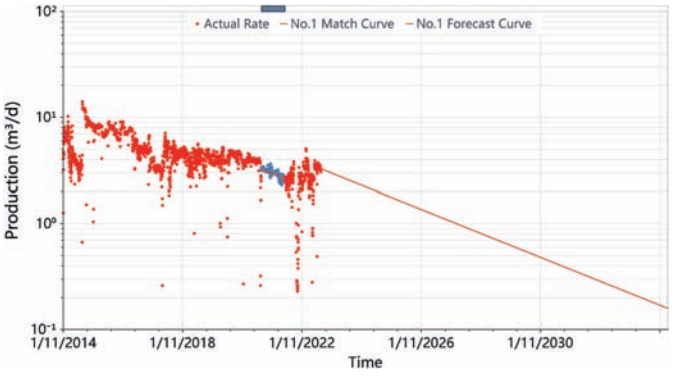


Fig. 6. Prediction of production in well A1 on the basis of hyperbolic decline.

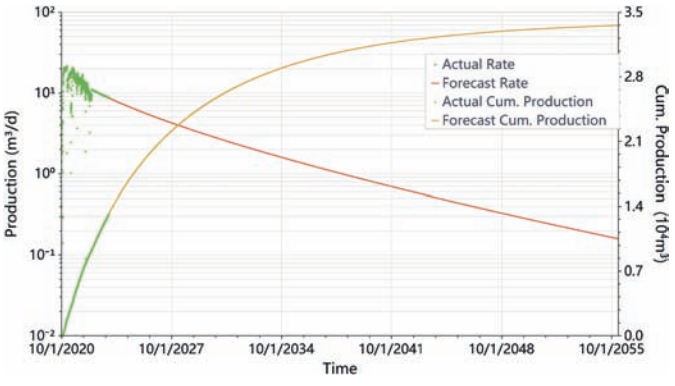


Fig. 7. Prediction of production in well A2 using Duong + YM-SEPD.

The regression equations are $y = 6.674x$, $3.4567x$, and $2.4416x$ for first one, two, and three years of production, respectively. The analysis showed that during the early production stage, the EUR exhibits a linear growth trend with increasing cumulative oil production in the wells. As production time increases, the slope of the linear regression equation between cumulative oil production and EUR decreases.

4.2. Relationship between cumulative oil production and EUR: Class II

Figs. 12–14 show the relationship between cumulative oil production at different periods and the empirical EUR of the Class II wells.

The regression equations are $y = 7.0558x$, $3.6402x$, and $2.5338x$ for first one, two, and three years of production, respectively.

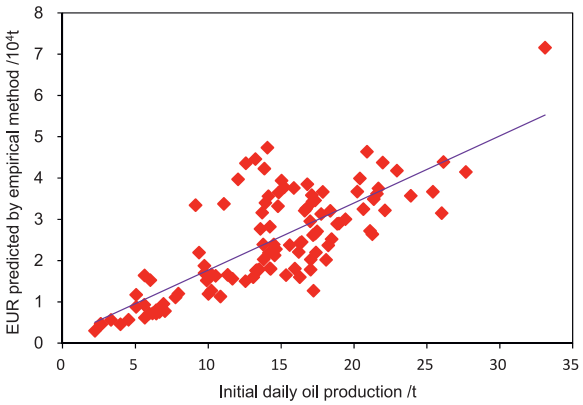


Fig. 8. Relationship between initial oil production and EUR.

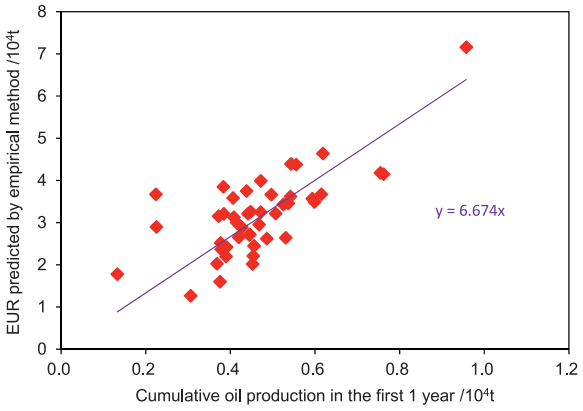


Fig. 9. Relationship between cumulative oil production over the first year and the empirical EUR of the Class I wells.

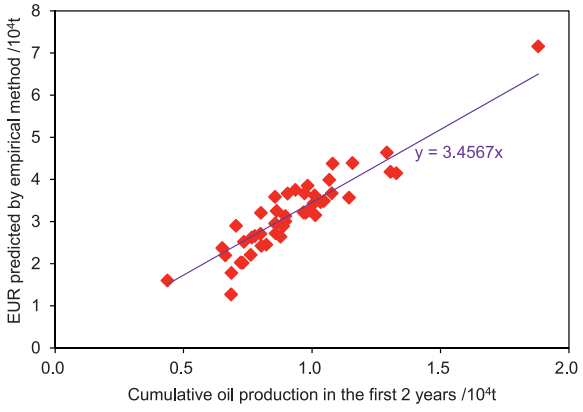


Fig. 10. Relationship between cumulative oil production over the first 2 years and the empirical EUR of the Class I wells.

Notably, the correlation between cumulative oil production and EUR is stronger after three years of production.

4.3. Relationship between cumulative oil production and EUR: Class III

Figs. 15–17 present the relationship between cumulative oil production at different periods and the empirical EUR of the Class

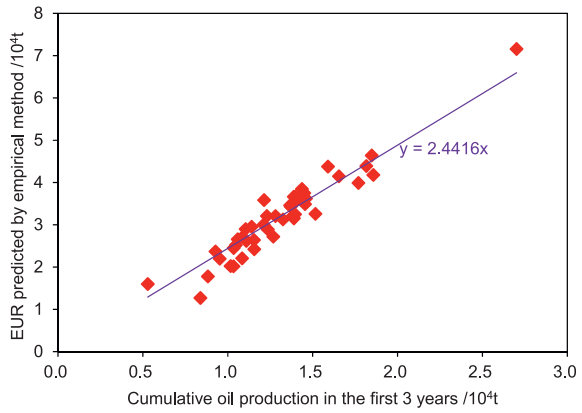


Fig. 11. Relationship between cumulative oil production over the first 3 years and the empirical EUR of the Class I wells.

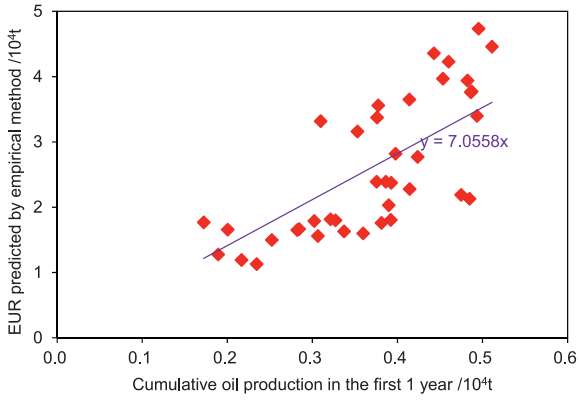


Fig. 12. Relationship between cumulative oil production over the first year and the empirical EUR of the Class II wells.

III wells. The regression equations are $y = 6.2708x$, $3.5104x$, and $2.4648x$ for first one, two, and three years of production respectively.

With Figs. 9–17 as bases, the correlation method for predicting the EUR of the X233 well zone in the Qingcheng Oil Field was developed (Table 2).

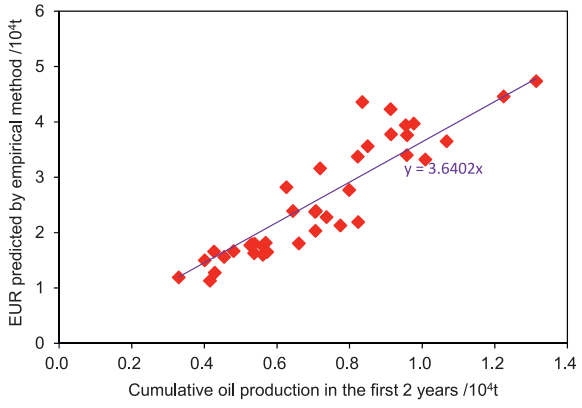


Fig. 13. Relationship between cumulative oil production over the first 2 years and the empirical EUR of the Class II wells.

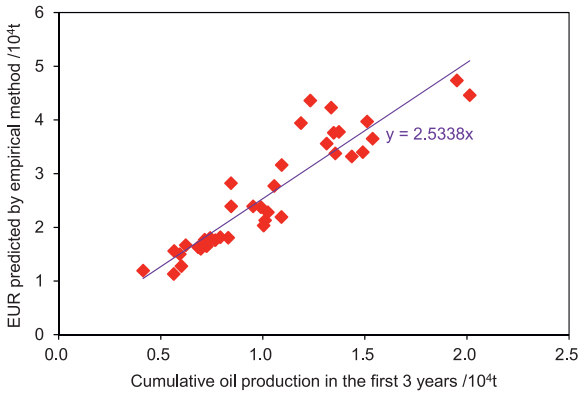


Fig. 14. Relationship between cumulative oil production over the first 3 years and the empirical EUR of the Class II wells.

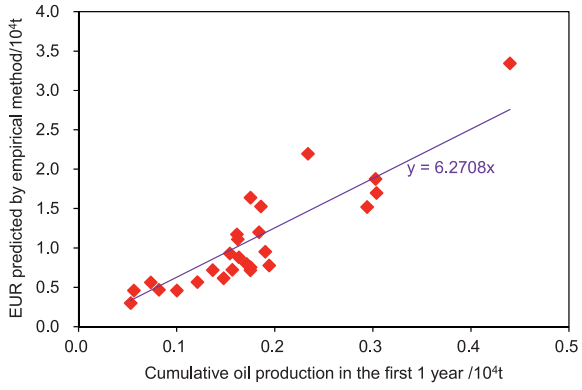


Fig. 15. Relationship between cumulative oil production over the first year and the empirical EUR of the Class III wells.

5. Adaptability analysis and application

5.1. Adaptability analysis of the correlation method

Table 3 compares the EUR values predicted using the empirical methods and the proposed correlation approach, along with their relative errors. The results indicated that the EUR values predicted by the correlation method are relatively close to those derived empirically, pointing to the favorable application effectiveness of

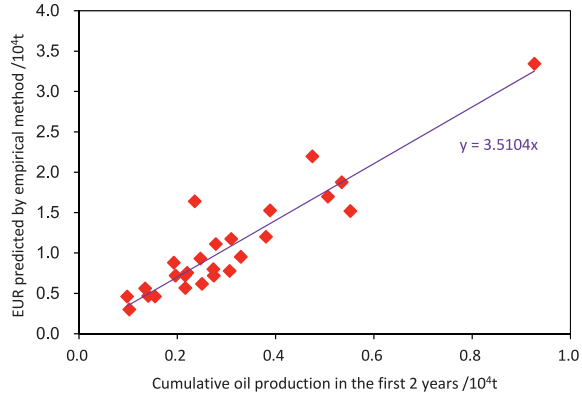


Fig. 16. Relationship between cumulative oil production over the first 2 years and the empirical EUR of the Class III wells.

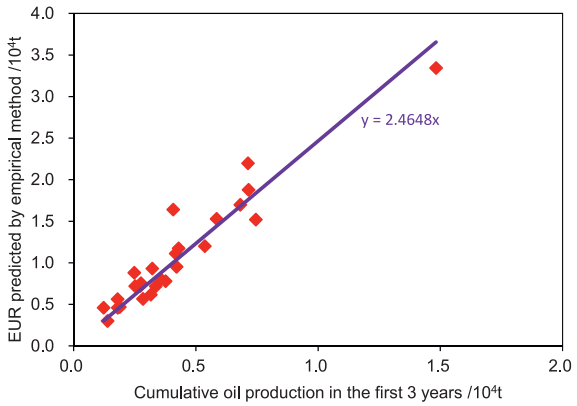


Fig. 17. Relationship between cumulative oil production over the first 3 years and the empirical EUR of the Class III wells.

the former. Additionally, the longer the production history of a single well, the higher the accuracy of the EUR predicted through the correlation method. This study recommends using a production history spanning at least two to three years.

For a single reservoir or block, the pore structure and reservoir fluids are relatively similar, and the production performance of the oil wells tends to follow comparable patterns. The proposed method uses the correlation between cumulative oil production and empirical EUR to predict. It simplifies conventional EUR calculation, thereby significantly reducing time and labor costs. However, its application requires the accurate calculation of the relationship equation, which depends on the quantity and quality of production data (e.g., the absence of long-term well shutdowns).

5.2. Case study

Wells B1, B2, and B3 were selected from Classes I, II, and III, respectively, for EUR prediction. In Well B1, the perforated interval extended from 2244.6 to 3836.0 m. Hydraulic fracturing was conducted in 22 stages, with the main purpose of improving hydrocarbon flow capacity in the target reservoir. Each fracturing stage was subdivided into several clusters, resulting in a total of 62 clusters. Here, each 'cluster' refers to a set of perforations within a fracturing stage, designed to enable more uniform distribution of fracturing fluid and more effective stimulation of the formation.

The fluid injection intensity was 16.82 m^3/m, while the sand injection intensity was 3.23 t/m. The well commenced operation in 2018, achieving an initial daily oil production of approximately 20.89 t. Its cumulative oil production after one, two, and three years of operation was 0.62 × 10^4 t, 1.29 × 10^4 t, and 1.85 × 10^4 t, respectively.

Well B2 was perforated at intervals of 2181.0–3128.0 m, with 12 fracturing stages. The fluid and sand injection intensities were 12.43 m^3/m and 1.22 t/m, respectively. The well began operating in 2018, realizing an initial daily oil production of approximately 11.07 t. Its cumulative oil production after one, two, and three years of operation was 0.38 × 10^4 t, 0.82 × 10^4 t, and 1.36 × 10^4 t, respectively.

In Well B3, perforations were made at intervals of 2343.00–3799.27 m, with 15 fracturing stages. The fluid injection intensity was 9.63 m^3/m, and the sand injection intensity was 1.50 t/m. The operation of the well was initiated in 2015, with an initial daily oil production of approximately 6.02 t. Its cumulative oil production after one, two, and three years of operation was 0.19 × 10^4 t, 0.39 × 10^4 t, and 0.58 × 10^4 t, respectively.

Table 2
The correlation method for predicting the EUR of the X233 well zone.

Class of wells	Number of wells	Initial oil rate/t (3 months after water cut is reduced to 60%)	Correlation method for predicting EUR y/10^4 t		
			x/10^4 t (Cumulative oil production in the first year)	x/10^4 t (Cumulative oil production in the first 2 years)	x/10^4 t (Cumulative oil production in the first 3 years)
Class I wells	45	$q_o > 16$ t	$y = 6.674x$	$y = 3.4567x$	$y = 2.4416x$
Class II wells	39	10 t < $q_o \leq 16$ t	$y = 7.0558x$	$y = 3.6402x$	$y = 2.5338x$
Class III wells	26	$q_o \leq 10$ t	$y = 6.2708x$	$y = 3.5104x$	$y = 2.4648x$

Table 3
EURs predicted by the empirical and correlation methods.

Class of well	Number of wells	Initial oil rate/t (3 months after water cut has been reduced to 60%)	Average EUR/10^4t (empirical method)	Average EUR/10^4 t (correlation method)			Relative error (%)		
				EUR predicted by cumulative oil production in the first year	EUR predicted by cumulative oil production in the first 2 years	EUR predicted by cumulative oil production in the first 3 years			
Class I wells	45	$q_o > 16$ t	3.18	3.114	3.203	3.201	2.08	0.74	0.67
Class II wells	39	10t < $q_o \leq 16$ t	2.58	2.617	2.613	2.583	1.42	1.28	0.11
Class III wells	26	$q_o \leq 10$ t	1.08	1.140	1.101	1.069	5.52	1.95	1.02

Table 4
Example calculations.

Well name	Initial oil rate/t (3 months after water cut has been reduced to 60%)	Average EUR/10^4 t (empirical method)	Average EUR/10^4 t (correlation method)			Relative error (%)		
			EUR predicted by cumulative oil production in the first year	EUR predicted by cumulative oil production in the first 2 years	EUR predicted by cumulative oil production in the first 3 years			
B1	20.89	4.64	4.13	4.46	4.51	11.04	3.82	2.76
B2	11.07	3.37	2.65	2.99	3.43	21.37	11.28	1.76
B3	6.02	1.53	1.17	1.37	1.44	23.68	10.59	5.64

The initial daily oil production of Well B1 is 20.89 t/d, which categorizes it as a Class I well. Its correlation-derived EURs and relative errors at years one, two, and three are 4.13×10^4 t, 4.46×10^4 t, and 4.51×10^4 t and 11.04%, 3.82%, and 2.76%, respectively. The initial daily oil production of Well B2 is 11.07 t/d, which warrants its categorization as a Class II well. Its correlation-predicted EURs and relative errors are 2.65×10^4 t, 2.99×10^4 t, and 3.43×10^4 t and 21.37%, 11.28%, and 1.76%, respectively. The initial daily oil production of Well B3 is 6.02 t/d, categorizing it as a Class III well. Its EURs and relative errors predicted via the correlation method are 1.17×10^4 t, 1.37×10^4 t, and 1.44×10^4 t and 23.68%, 10.59%, and 5.64%, respectively. These details are listed in Table 4.

6. Conclusion

As previously stated, the production of Qingcheng shale oil can be divided into the production ramp-up, rapid decline (annual oil production decline ~20.8%), and slow decline (annual oil production decline ~11.5%) stages. The EUR is linearly correlated with the initial daily oil production of a well: The greater the initial daily oil production, the higher the EUR. The average EURs of Classes I, II, and III are 3.18×10^4 t, 2.58×10^4 t, and 1.08×10^4 t, respectively.

The relationship between cumulative oil production and empirical EUR was used as a basis for establishing the correlation method for predicting EUR. The accuracy of EUR predictions improves as more years are encompassed by the production history of a single well. This research suggests a production history that spans at least two to three years when predicting EURs using the proposed correlation approach. The production conditions of a well itself can also affect the accuracy with which EURs are predicted via the correlation method. For example, long-term well shutdowns or multiple workover operations may cause deviations in predicted EURs. In such cases, it is advisable to derive the average of predictions obtained through multiple calculations. Meanwhile, given its reliance on minimal, early production data, this approach is readily transferable to other countries with similar geological settings or at early stages of shale oil development, such as North America and emerging unconventional resource areas. It can help operators in these regions rapidly assess well performance, optimize investment strategies, and mitigate uncertainties associated with limited data availability.

CRediT authorship contribution statement

Suiyi Fu: Methodology, Formal analysis, Data curation, Conceptualization. **Lingbin Lai:** Methodology, Investigation, Data curation. **Zhengdong Lei:** Methodology, Formal analysis, Data curation. **Qingfu Feng:** Resources, Methodology, Investigation, Data curation. **Huizhu Xiang:** Methodology, Investigation, Formal analysis, Data curation, Conceptualization. **Bo Wang:** Resources, Methodology. **Xiulin Hou:** Methodology, Data curation. **Ting Xue:** Data curation.

Declaration of competing interest

The authors declare that there is no conflict of interest.

References

Acuña, J.A., 2021. A physically consistent decline analysis method for unconventional wells. In: Paper Presented at the Unconventional Resources Technology Conference (URTeC). https://doi.org/10.15530/urtec-2021-5096. Houston, Texas, USA.

Arps, J.J., 1945. Analysis of decline curves. Trans. AIME 160 (1), 228–247. https://doi.org/10.2118/945228-G.

Artus, V., Houzé, O., 2018. A physical decline curve for fractured horizontal wells. In: Paper Presented at the Unconventional Resources Technology Conference (URTeC). https://doi.org/10.15530/URTEC-2018-2856750. Houston, Texas, USA.

Clark, A.J., Lake, L.W., Patzek, T.W., 2011. Production forecasting with logistic growth models. In: Paper Presented at the SPE Annual Technical Conference and Exhibition. https://doi.org/10.2118/144790-MS. Denver, Colorado, USA.

Duong, A.N., 2010. An unconventional rate decline approach for tight and fracture-dominated gas wells. In: Paper Presented at the Canadian Unconventional Resources and International Petroleum Conference. https://doi.org/10.2118/137748-MS. Calgary, Alberta, Canada.

Duong, A.N., 2011. Rate-decline analysis for fracture-dominated shale reservoirs. SPE Reservoir Eval. Eng. 14 (3), 377–387. https://doi.org/10.2118/137748-PA.

Ei-Banbi, A.H., Wattenbarger, R.A., 1998. Analysis of linear flow in gas flow production. In: Proceedings of the SPE Gas Technology Symposium. https://doi.org/10.2118/39972-MS. Calgary, Alberta, Canada, SPE-39972.

Hui, P., Qiquan, R., Yong, L., Min, T., 2017. Performance analysis and flow regime identification of fractured horizontal wells in tight oil reservoirs. In: Paper Presented at the SPE Kingdom of Saudi Arabia Annual Technical Symposium and Exhibition. https://doi.org/10.2118/188071-MS. Dammam, Saudi Arabia, SPE-188071-MS.

Ibrahim, A.F., Alarifi, S.A., Elkatatny, S., 2023. Retracted article: data-driven EUR for multistage hydraulically fractured wells in shale formation using different machine learning methods. J. Pet. Explor. Prod. Technol. 13, 1123–1134. https://doi.org/10.1007/s13202-022-01602-1.

Joshi, K., Lee, J., 2013. Comparison of various deterministic forecasting techniques in shale gas reservoirs. In: Paper Presented at the SPE Hydraulic Fracturing Technology Conference. https://doi.org/10.2118/163870-MS. The Woodlands, Texas, USA.

Ju, W., Liang, Y., Feng, S., Xin, H., You, Y., Ning, W., Yu, G., 2023. Brittleness assessment of the shale oil reservoir based on neural network method: a case study of the Yanchang Formation, Ordos Basin. Unconv. Resour. 3, 54–60.

Kabir, C.S., Rasdi, F., Igboalisi, B., 2011. Analyzing production data from tight oil wells. J. Can. Petrol. Technol. 50 (5), 48–58. https://doi.org/10.2118/146818-PA.

Li, F., 2013. Study on Productivity Decline Rule in Low Permeability Reservoir. Master's thesis. Xi'an Petroleum University, Xi'an, China.

Mehana, M., Callard, J., Mansi, M., Gong, Y., 2019. Integrating production analysis with Monte Carlo simulation for estimated ultimate recovery EUR prediction. In: Paper Presented at the SPE Eastern Regional Meeting. https://doi.org/10.2118/196603-MS. Charleston, West Virginia, USA.

Niu, X., Feng, S., You, Y., Xin, H., Liang, X., Hao, B., Dan, W., 2022. Analyzing major controlling factors of shale oil 'sweet spots' in the Chang-7 member of the Triassic Yanchang Formation, Ordos Basin. Unconv. Resour. 2, 51–59.

Patzek, T.W., Male, F., Marder, M., 2013. Gas production in the Barnett Shale obeys a simple scaling theory. Proc. Natl. Acad. Sci. U. S. A 110 (49), 19731–19736. https://doi.org/10.1073/pnas.1313380110.

Ruiz Maraggi, L.M., Walsh, M.P., Lake, L.W., 2024. A new approach to apply decline-curve analysis for tight-oil reservoirs producing under variable pressure conditions. SPE J. 29, 1655–1671. https://doi.org/10.2118/218016-PA.

Seidle, J.P., Joshi, V., Gustason, E., 2016. Estimating developed reservoirs in selected low-permeability unconventional reservoirs. In: SPEE Monograph Series No.4, Society of Petroleum Evaluation Engineers. Houston, TX.

Statton, J.C., 2011. Application of the Stretched Exponential Production Decline Model to Forecast Production in Shale Gas Reservoir. MS Thesis. Texas A&M University, College Station, TX, USA.

Temizel, C., Canbaz, C.H., Balaji, K., Ozesen, A., Yanidis, K., Alsaheib, H., AlSulaiman, N., Basri, M., 2021. Hybrid modeling in unconventional reservoirs to forecast estimated ultimate recovery. In: Paper Presented at the Offshore Technology Conference. https://doi.org/10.4043/31010-MS. Houston, Texas, USA.

Valko, P.P., 2009. Assigning value to stimulation in the Barnett Shale: a simultaneous analysis of 7000 plus production histories and well completion records. In: Paper Presented at the SPE Hydraulic Fracturing Technology Conference. https://doi.org/10.2118/119369-MS. The Woodlands, Texas, USA, SPE-119369.

Wang, J., Wei, Y., Qi, Y., Ni, J., Yu, W., Yuan, H., Zhu, H., Lei, D., 2022. A new integrated decline prediction model based on Bayesian inference. Nat. Gas. Ind. 42 (11), 77–87.

Wattenbarger, R.A., Ei-Banbi, A.H., Villegas, M.E., Maggard, J.B., 1988. Production analysis of linear flow into fractured tight gas wells. In: Proceedings of the SPE Unconventional Gas Technology Symposium. https://doi.org/10.2118/39931-MS. Pittsburgh, Pennsylvania, USA, SPE-39931.

Xue, T., Huang, T., Cheng, L., Ma, S., Shi, J., 2021. Dominating factors on shale oil horizontal well productivity and development strategies optimization in Qingcheng Oilfield, Ordos Basin. Nat. Gas Geosci. 32 (12), 1880–1888. https://doi.org/10.11764/j.issn.1672-1926.2021.12.1880.

Yu, S., 2013. Best practice of using empirical methods for production forecast and EUR estimation in tight/shale gas reservoirs. In: Paper Presented at the SPE Unconventional Resources Conference Canada. https://doi.org/10.2118/167118-MS. Calgary, Alberta, Canada, SPE-167118-MS.

Yu, S., 2018. Engineering Methods for Shale and Tight Oil and Gas Reservoirs. Petroleum Industry Press, Beijing, China.

Yu, S., Jiang, Z., Lee, W.J., 2018. Reconciling empirical methods for reliable EUR and production profile forecasts of horizontal wells in tight/shale reservoirs. In: Proceedings of the SPE Canada Unconventional Resources Conference. https://doi.org/10.2118/189802-MS. Calgary, Alberta, Canada, SPE-189802-MS.

Zhang, J., Bi, H., Xu, H., Zhao, J., Zhao, D., Geng, J., 2016. Applicability of the predicting method for the oil and gas production and their reservoirs in the tight reservoirs. Pet. Geol. Oilfield Dev. Daqing 35 (3), 151–158.